Bull. Chem. Soc. Ethiop. **2013**, 27(2), 273-280. ISSN 1011-3924
Printed in Ethiopia

DOI: http://dx.doi.org/10.4314/bcse.v27i2.12

N,N′-DIPYRIDOXYL(1,8-DIAMINO-3,6-DIOXAOCTANE) SCHIFF-BASE: SYNTHESIS, EXPERIMENTAL AND THEORETICAL IDENTIFICATION

S. Ali Beyramabadi[1,*], Ali Morsali[1], Mohammad Reza Bozorgmehr[1], Malihe Javan Khoshkholgh[2] and Abbas Ali Esmaeili[2]

[1]Department of Chemistry, Mashhad branch, Islamic Azad University, Mashhad, Iran
[2]Department of Chemistry, School of Sciences, Ferdowsi University of Mashhad, Mashhad 91775-1436, Iran

(Received November 14, 2011; revised January 14, 2013)

ABSTRACT. The N,N′-dipyridoxyl(1,8-diamino-3,6-dioxaoctane) (=H_2L) Schiff-base has been synthesized and characterized by IR, ^1H NMR, mass spectrometry and elemental analysis. Its optimized geometry and theoretical vibrational frequencies have been computed using density functional theory (DFT) method *via* the B3LYP functional. Also, its ^1H and ^{13}C NMR chemical shifts have been calculated at the same computational level. In optimized geometry of the H_2L, the two pyridine rings are perpendicular to each other. The phenolic hydrogens are engaged in intramolecular-hydrogen bonds with the azomethine nitrogens.

KEY WORDS: Schiff base, N,N′-dipyridoxyl(1,8-diamino-3,6-dioxaoctane), DFT, B3LYP

INTRODUCTION

Schiff bases due to structural varieties and unique characteristics are the most versatile studied ligands in coordination chemistry [1, 2] and their metal complexes play an important role in the development of inorganic chemistry [3].

A variety of applications, including biological [4, 5], analytical [6, 7] and industrial use as catalysts [8, 9], make the Schiff-base ligands and their complexes to be of great importance. It has been shown that the chain length of Schiff bases influences catalytic activity of their complexes [10].

With the continuation of our studies [11-13], here we report the synthesis and experimental characterization of the N,N′-dipyridoxyl(1,8-diamino-3,6-dioxaoctane) (=H_2L) Schiff bases, where the 1,8-diamino-3,6-dioxaoctane moiety acts as a bridge between two dipyridoxyl groups. In addition, geometries optimization and theoretical assignment of the IR, ^1H and ^{13}C NMR spectra of the H_2L have been performed by using DFT method, which is widely used as a remarkable method in many areas of the computational chemistry [11-20].

EXPERIMENTAL

Materials and methods

All of used chemicals and solvents were purchased from Merck except for pyridoxal hydrochloride which was obtained from Fluka. They were used as received. Melting points were measured by using an Electrothermal 9100 melting point apparatus. Elemental analysis (C, H, N) was made on a Heraeus elemental analyzer CHN-O-Rapid. The IR spectra were recorded with a PerkinElemer 783 infrared spectrophotometer. Mass spectra were recorded on a Shimadzu-GC-Mass-Qp 1100 Ex. The NMR spectra were recorded in $(CD_3)_2CO$ on a Bruker Drx-500 Avance spectrometer (500.13 MHz).

---

*Corresponding author. E-mail: beiramabadi6285@mshdiau.ac.ir

Synthesis of the H_2L

Pyridoxal hydrochloride (611 mg, 3 mmol) was dissolved in 5 mL of methanol, and then was added to methanolic Et_3N (303 mg, 3 mmol in 5 mL). This mixture was stirred for a few min. Then, a methanolic solution of 1,8-diamino-3,6-dioxaoctane (669 mg, 1.5 mmol in 5 mL) was slowly added to the mixture, which resulted in synthesis of the H_2L. The mixture was stirred for 5 h. The orange solid was filtered, washed with cold methanol and dried in air (yield: 30%. decomp. 155 °C).

Computational methods

All the calculations were performed by using the gradient-corrected DFT method with the B3LYP functional [21] and at 6-31+G(d,p) basis sets. The Gaussian 03 program package [22] was used with its default procedures. Geometry of the H_2L was fully optimized, where the optimized geometry was confirmed to have no imaginary frequency of the Hessian. Then, the gas phase optimized geometry was used to compute theoretical vibrational frequencies of the H_2S species. Also, its ^1H and ^{13}C NMR chemical shifts were predicted with respect to tetramethylsilane (TMS), where the GIAO method was used for prediction of the DFT nuclear shieldings [23].

RESULTS AND DISCUSSION

Geometry optimization

In this work, structural parameters of the H_2L species were determined, important of which are gathered in Table 1. For comparison, some structural parameters of the similar compounds are listed in Table 1. The DFT structural parameters of H_2L are in agreement with the structural data reported for the similar Schiff-bases [1, 2, 10-13, 24-40], confirming validity of the optimized geometry for the H_2L Schiff-base. The optimized geometry of the H_2L with atom labelling is shown in Figure 1. In the non-planar geometry of the H_2L, two pyridine rings are in a separate plane, approximately perpendicular to each other. The pyridine rings are essentially planar; all the substitutions are in the same plane with the corresponding pyridine rings, too.

The calculated bond lengths are in the expected range. As expected, the phenolic C1-O1 and C2-O9 bond lengths (134.0 pm) are shorter than both the alcoholic (142.1 pm) and etheric (142) ones. On the other hand, the alcoholic O-H bonds (96.7 pm) are shorter than the phenolic ones (100.0 pm). The phenolic hydrogens are engaged in the intramolecular-hydrogen-bond interactions with the azomethine-nitrogen atoms, which elongates the phenolic O-H bonds in comparison with the alcoholic ones. Formation of the intramolecular-hydrogen bond generates six-membered rings. The N...OH and N…O hydrogen bond distances are 169.9 and 259.5 pm, respectively, showing strong hydrogen bond interaction. This interaction decreases the electron density in the binding region of the phenolic O-H bonds. The calculated parameters for the H_2L are in well agreement with the previously reported values for the similar compounds [1, 2, 10-13, 24-40], confirming validity of the optimized geometry for the H_2L species.

In this work, the electron populations of the frontier orbitals have been calculated by using the natural bond orbital (NBO) analysis at the B3LYP/6-31+G(d,p) level. The calculated 3-D maps of the highest occupied molecular orbital (HOMO) and lowest unoccupied molecular orbital (LUMO) are shown in Figure 2. As seen, electron clouds of the HOMO orbital are located on the pyridine rings and phenolic oxygens, while the LUMO orbital is located on the π^* orbital of the C=N azomethine groups.

Table 1. Selected calculated structural parameters of H_2L in comparison with the similar compounds.

Structural parameters	Similar compounds	H_2L
Bond lengths (pm)		
C1-O1	134.1 [16]; 132.0 [28]; 131.6 [29]; 131.1 [30]; 134.1 [36]; 136.1 [37]	134.4
C1-C2	141.8 [16]; 141.2 [30]; 142.5 [33]; 141.0 [37]	141.9
C2-N3	132.8 [16]; 132.5 [38]; 133.8 [39]	133.0
N3-C3	134.8 [16]; 133.6 [38]; 133.8 [39]; 134.0 [40]	134.9
C2-C6	150.4 [16]; 153.9 [37]; 151.0 [40]	150.4
C4-C7	152.2 [16]; 152.1 [38]; 151.6 [39]	152.3
C7-O3	142.0 [16]; 141.9 [38]; 141.2 [39]	142.1
C5-C8	145.9 [16]; 144.2 [30]; 143.6 [32]; 143.6 [33]; 145.0 [36]; 145.2 [37]	146.1
C8-N1	128.7 [16]; 129.0 [28]; 129.9 [29]; 128.8 [30]; 128.2 [32]; 128.7 [33]	128.7
O1-H1	100.0 [16]; 98.9, 103.5 [37]	100.0
N1-H1	169.1 [16]	170.0
N1-O1	259.5 [16]	260.0
O3-H9	96.7 [16]; 96.1 [39]	96.7
C3-H3	108.5 [16]; 107.0 [37]; 108.0, 100.0 [38]	108.5
C8-H10	109.6 [16]; 103.8, 107.2 [29]	109.7
N1-C17	147.7 [28]; 148.2 [29]; 148.0 [33]; 146.1 [36]; 147.6 [37]	145.3
C17-C18		152.9
C19-O5		141.8
Angles (°)		
H1-O1-C1	106.9 [16]; 113.1 [36]; 103.4, 104.6 [37]	107.4
O1-C1-C5	122.6 [16]; 123.7 [31]; 123.7 [32]; 121.2 [36]	122.5
C1-C5-C8	119.9 [16]; 121.2 [32]; 121.6 [36]; 121.1 [37]; 120.8 [39]	120.0
C2-N3-C3	119.4 [16]; 117.5 [39]; 119.9 [40]	119.6
C5-C8-N1	122.2 [16]; 122.9 [29]; 122.5 [30]; 122.5 [36]; 123.5 [37]	122.3
C1-O1-O2	76.1 [16]; 163.4 [29]; 15.9 [31]; 7.3 [33]; 84.9 [36]	127.5
Dihedral angles (°)		
H1-O1-C1-C5	0.7 [16]; 5.2 [37]	0.3
O1-C1-C5-C8	-0.7 [16]; -3.2, 0.7 [29]; -1.8, -2.2 [30]; -1.1, -2.0 [33]; -1.5, -1.9 [36]; -2.47 [37]	-0.7
C1-C2-N3-C3	0.3 [16]; -0.2 [38]; -0.7, -0.2 [39]	0.4
C1-C5-C4-C7	179.5 [16]	-179.7
C1-C5-C8-N1	0.5 [16]; -1.7 [29]; 2.6 [30]; 9.8 [31]; 2.0, 10.6 [33]; 0.9 [36]; 2.9, -6.6 [37]	0.5
O1-N1-N2-O2	105.4 [16]; 1.2 [29]; 1.9 [30]; -1.5 [33]; 33.6 [36]; -79.7 [37]	-103.9
C3-C1-C9-C11	-90.5 [16]; -20.4 [36]; 121.5 [37]	-73.2
C1-O1-O2-C9	94.0 [16]; 176.3 [31]; 169.8 [33]	-79.7

Elemental analysis and mass spectrometry

The elemental analysis results for the H_2L species confirm the proposed formula. Anal. calc. for $C_{22}H_{30}N_4O_6$: C, 59.2 %; H, 6.8 %; N, 12.6 %. Found: C, 59.4 %; H, 6.4 %; N, 13.1 %. Also, the decomposition mass losses of the H_2L (MS: m/z (%) 445 (M^+)) were found in consistent with the proposed formula.

NMR spectra

The experimental and theoretical ^1H and ^{13}C NMR chemical shifts (δ) of the H_2L Schiff-base are given in Table 2, where the atom positions are numbered as in Figure 1. The appearance of a signal at 13.8 ppm is assigned to the phenolic protons (H1, H2), where their engagement in the intramolecular hydrogen bond interaction (O-H…N), shifts their signals to upfield [23, 41].

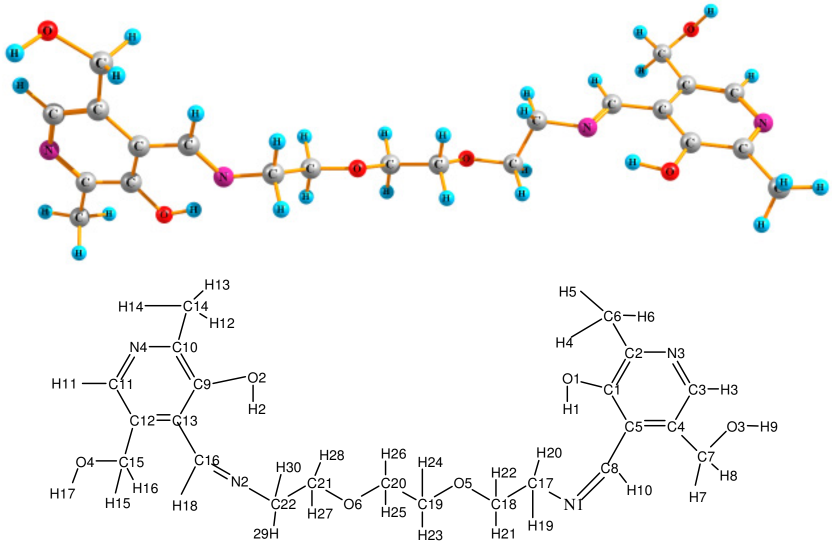

Figure 1. Structure and B3LYP optimized geometry of the N,N′-dipyridoxyl(1,8-diamino-3,6-dioxaoctane) together with its atom labelling.

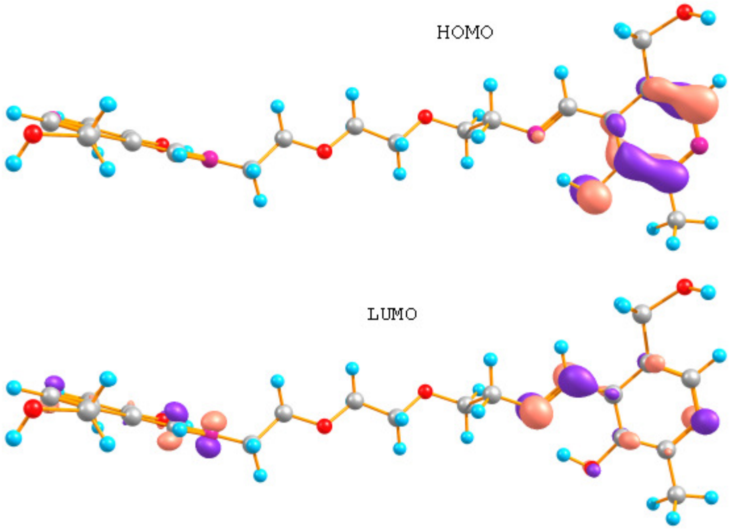

Figure 2. The HOMO and LUMO frontier orbitals of the N,N′-dipyridoxyl(1,8-diamino-3,6-dioxaoctane).

Table 2. Experimental and theoretical ^1H- and ^{13}C-NMR chemical shifts of N,N′-dipyridoxyl(1,8-diamino-3,6-dioxaoctane) in $(CD_3)_2CO$ solution, δ [ppm].

^1H NMR						^{13}C NMR					
Atom position	Exp.	Theo.	Atom position	Exp.	Theo.	Atom position	Exp.	Theo.	Atom position	Exp.	Theo.
H1	13.8	14.1	H28	3.8	4.7	C8	163.7	148.2	C20	69.6	59.2
H2	13.8	14.1	H21	3.6	4.6	C16	163.7	148.0	C17	69.5	53.4
H10	8.9	9.4	H22	3.6	4.6	C1	156.1	140.7	C22	69.5	53.4
H18	8.9	9.4	H25	3.6	4.6	C9	156.1	140.6	C7	58.5	51.8
H3	7.8	9.2	H26	3.6	4.4	C2	149.5	137.5	C15	58.5	51. 8
H11	7.8	9.2	H30	3.8	4.1	C10	149.5	137.5	C8	57.6	51.3
H8	4.7	6.0	H19	3.8	3.8	C3	135.5	120.4	C16	57.6	51.3
H15	4.7	6.0	H4	2.4	3.4	C11	135.5	120.2	C6	16.7	12.3
H16	4.7	5.8	H5	2.4	3.4	C4	132.6	119.4	C14	16.7	12.3
H7	4.7	5.8	H12	2.4	3.4	C12	132.6	119.3			
H20	3.8	5.3	H13	2.4	3.4	C5	119.3	103.8			
H29	3.8	5.1	H6	2.4	3.0	C13	119.3	103.6			
H24	3. 8	4.9	H14	2.4	3.0	C18	69.6	62.1			
H27	3.8	4.7	H9	4.8	0.7	C21	69.6	62.0			
H23	3.8	4.7	H17	4.8	0.7	C19	69.6	60.5			

The calculated chemical shifts are in good agreement with the experimental values, confirming suitability of the optimized geometry for the H_2L species. The only exception is the chemical shift of the alcoholic protons (H9 and H17), where their experimental chemical shifts are significantly higher than the calculated ones. The experimental data are from $(CD_3)_2CO$ solutions but the calculations correspond to the isolated molecule in the gas phase. Obviously, the solvent molecules interact with the alcoholic proton. Also, the alcoholic protons may engage in intermolecular hydrogen bonds.

Vibrational spectroscopy

Theoretical investigation of the IR and NMR spectra could be used as an important tool for identification of chemical species, especially evaluation of proposed geometries for compounds with undeterminated X-ray structure [10-14, 42]. The selected DFT vibrational frequencies of the H_2L are listed in Table 3. The vibrational modes were analyzed by comparing the previously reported data [28, 30-32] with the present work.

In the 3600-2000 cm^{-1} spectral region of the IR spectra, overlapping of stretching vibrations of the O-H bonds with each other and with the C-H stretching modes causes to a band broadening [10-13, 32, 33]. In Table 3, deconvolution of this region is given, where the most intensive band is related to the stretching vibrations of the phenolic O-H bonds. These vibrations are appeared at lower energies than the alcoholic O-H ones.The very intensive bands at 1660-1500 cm^{-1} region accounts as an important band in the infrared spectra of the Schiff-bases [10-13, 43-45]. Here, a very intensive band at 1641 cm^{-1} region of the IR spectrum is attributed to the symmetrical stretching modes of C8=N1 and C16=N2 bonds. Vibrational modes of the bridge region causes to appearance of some absorption bands, important of which are assigned in Table 3.

Table 3. Selected experimental and calculated IR vibrational frequencies (cm^{-1}) of the H_2L.

Experimental frequencies	Calculated		Vibrational assignment
	Frequencies	Intensity	
731 (w)	731	20	Breathing of pyridine ring
892 (m)	891	83	$\delta_{oot\text{-}of\text{-}plane}$(O-H) phenolic
998 (s)	1027	23	ν_{sym}(C-O-C) ether
1041 (s)	1075	50	δ(CH) Me[a] + ν(C-O) alc[b] + ν(C17-N1, C16-N2)
1136 (s)	1162	472	ν_{asym}(C-O-C) ether
1197 (m)	1246	49	ν(ph-C)+ ν(C1-C2, N3-C3, C4-C5, C9-C10, N4-C11, C12-C13)
1271 (s)	1314	53	$\delta_{wagging}$(CH_2) bridge[c]
1314 (s)	1399	63	[$\delta_{twisting}$ (CH_2)+ $\delta_{in\text{-}planep}$(OH)] alc[b]
1406 (vs)	1439	108	ν(C1-O1) + ν(C9-O2) + ν(ph ring)+ ν(ph-C)+ ν(C9-O2) + ν(ph ring))+ ν(ph-C) right[e]
1641 (vs)	1692	189	ν(C8-N1), ν(C16-N2)
2896 (s)	2984, 2999	28,59	ν_{sym}(CH) bridge
	3004	74	ν_{sym}(CH) alc[b]
2928 (sh)	3024	47	ν_{asym}(CH) bridge[c]
	3043	20	ν_{sym}(CH) Me[a]
2948 (sh)	3053	74	ν_{asym}(CH) bridge[c]
	3063	91	$\nu(C_8H_{10})+\nu(C_{16}\text{-}H_{18})$
	3071	13	ν_{asym}(CH) alc[b]
3148 (br, s)	3075	22	ν_{asym}(CH) bridge[c]
	3096	13	ν_{asym}(CH) Me[a]
	3102	35	ν_{asym}(CH) bridge[c]
	3122,3124	708,296	ν(O-H) phenolic
	3208	7	ν(C-H) aromatic
	3814	32	ν(O-H) alc[b]

Abbreviation: a: substituted $–CH_3$ groups; b: substituted $–CH_2OH$ groups; c: N1-bridge region of molecule-N2; d: left side of the molecule; e: right side of the molecule; w, weak; m, medium; s, strong; vs, very strong; sh, shoulder; br, broad.

CONCLUSION

In this work, we have synthesized and characterized a new Schiff-base (H_2L). The geometry optimization, ^1H and ^{13}C NMR chemical shifts and IR vibrational frequencies of the H_2L have been calculated using DFT methods. The calculated results are in agreement with the experimental evidence, confirming validity of the optimized geometry for the H_2L.

The H_2L molecule is not planar, but two pyridine rings are roughly perpendicular to each other. However, the substituents are in a same plane with the pyridine rings. The intramolecular hydrogen bonds between the phenolic protons and the azomethine nitrogens changes chemical shifts of the phenolic protons to 13.8 ppm in the ^1H NMR spectrum of the free H_2L ligand. In addition, important IR vibrational frequencies of the H_2L have been assigned using DFT calculations. The obtained results could be used for identification of similar compounds.

REFERENCES

1. Yu, D.; Xiaoxia, H.; Xiaoli, S.; Zhiling, Z. *Wuhan Univ. J. Nat. Sci.* **2010**, 15, 165.
2. Kumar, D.; Gupta, P.K.; Syamal, A. *J. Chem. Sci.* **2005**, 117, 247.

3. Valent, A.; Melník, M.; Hudecová, D.; Dudová, B.; Kivekäs, R.; Sundberg, M.R. *Inorg. Chim. Acta* **2002**, 340, 15.
4. Lamour, E.; Routier, S.; Bernier, J.L.; Catteau, J.P.; Bailly, C.; Vezin, H. *J. Am. Chem. Soc.* **1999**, 121, 1862.
5. Morrow, J.R.; Kolasa K. *Inorg. Chim. Acta* **1992**, 195, 245.
6. Sadeghi, S.; Gafarzadeh, A.; Naeimi, H. *J. Anal. Chem.* **2006**, 61, 677.
7. Dadfarnia, S.; Haji Shabani, A.M.; Tamadon, F.; Rezaei, M. *Microchim. Acta* **2007**, 158, 159.
8. Sakthivel, A.; Sun, W.; Raudaschl-Sieber, G.; Chiang, A.S.T.; Hanzlik, M.; Kühn, F.E. *Catal. Commun.* **2006**, 7, 302.
9. Gupta, K.C., Sutar, A.K. *J. Mol. Catal. A: Chem.* **2007**, 272, 64.
10. Gupta, K.C.; Sutar, A.K. *Coord. Chem. Rev.* **2008**, 252, 1420.
11. Eshtiagh-Hosseini, H.; Housaindokht, M.R.; Beyramabadi, S.A.; Beheshti, S.; Esmaeili, A.A.; Javan-Khoshkholgh, M.; Morsali, A. *Spectrochim. Acta Part A* **2008**, 71, 1341.
12. Eshtiagh-Hosseini, H.; Housaindokht, M.R.; Beyramabadi, S.A.; Mir Tabatabaei, S.H.; Esmaeili, A.A.; Javan-Khoshkholgh, M. *Spectrochim. Acta Part A* **2011**, 78, 1046.
13. Beyramabadi, S.A.; Morsali, A.; Javan-Khoshkholgh, M.; Esmaeili, A.A., *J. Struct. Chem.* **2011**, 53, 460.
14. Eshtiagh-Hosseini, H.; Aghabozorg, H.; Mirzaei, M.; Beyramabadi, S.A.; Eshghi, H.; Morsali, A.; Shokrollahi, A.; Aghaei, R. *Spectrochim. Acta Part A* **2011**, 78, 1392.
15. Beyramabadi, S.A.; Eshtiagh-Hosseini, H.; Housaindokht, M.R.; Morsali, A. *Organometallics* **2008**, 27, 72.
16. Beyramabadi, S.A.; Eshtiagh-Hosseini, H.; Housaindokht, M.R.; Morsali A. *J. Mol. Struct.: THEOCHEM* **2009**, 903, 108.
17. Alkorta, I.; Elguero, J.; Roussel C. *Comput. Theor. Chem.* **2011**, 966, 334.
18. Alver, Ö.; Parlak, C.; Bilge, M. *Bull. Chem. Soc. Ethiop.* **2011**, 25, 437.
19. Alver, Ö.; Parlak, C.; Şenyel, M. *Bull. Chem. Soc. Ethiop.* **2009**, 23, 85.
20. Vessally, E. *Bull. Chem. Soc. Ethiop.* **2008**, 22, 465.
21. Lee, C.; Yang, W.; Parr, R.G. *Phys. Rev. B* **1988**, 37, 785.
22. Frisch, M.J.; Trucks, G.W.; Schlegel, H.B.; Scuseria, G.E.; Robb, M.A.; Cheeseman, J.R.; Montgomery, J.A.; Vreven, T.; Kudin, K.N.; Burant, J.C.; Millam, J.M.; Iyengar, S.S.; Tomasi, J.; Barone, V.; Mennucci, B.; Cossi, M.; Scalmani, G.; Rega, N.; Petersson, G.A.; Nakatsuji, H.; Hada, M.; Ehara, M.; Toyota, K.; Fukuda, R.; Hasegawa, J.; Ishida, M.; Nakajima, T.; Honda, Y.; Kitao, O.; Nakai, H.; Klene, M.; Li, X.; Knox, J.E.; Hratchian, H.P.; Cross, J.B.; Bakken, V.; Adamo, C.; Jaramillo, J.; Gomperts, R.; Stratmann, R.E.; Yazyev, O.; Austin, A.J.; Cammi, R.; Pomelli, C.; Ochterski, J.W.; Ayala, P.Y.; Morokuma, K.; Voth, G.A.; Salvador, P.; Dannenberg, J.J.; Zakrzewski, V.G.; Dapprich, S.; Daniels, A.D.; Strain, M.C.; Farkas, O.; Malick, D.K.; Rabuck, A.D.; Raghavachari, K.; Foresman, J.B.; Ortiz, J.V.; Cui, Q.; Baboul, A.G.; Clifford, S.; Cioslowski, J.; Stefanov, B.B.; Liu, G.; Liashenko, A.; Piskorz, P.; Komaromi, I.; Martin, R.L.; Fox, D.J.; Keith, T.; Al-Laham, M.A.; Peng, C.Y.; Nanayakkara, A.; Challacombe, M.; Gill, P.M.W.; Johnson, B.; Chen, W.; Wong, M.W.; Gonzalez, C.; Pople, J.A., *Gaussian 98, Revision A.7*, Gaussian, Inc.: Pittsburgh PA; **1998**.
23. Ditchfield, R. *Mol. Phys.* **1974**, 27, 789.
24. Kumari, D.; Syamal, A.; Jaipal, Kumar Sharma, L. *J. Chem. Sci.* **2009**, 121, 57.
25. Deters, R.; Krämer, R. *Inorg. Chim. Acta* **1998**, 269, 117.
26. Al-Jeboori, M.J.; Hasan, H.A.; Al-Sa'idy, W.A.J. *Transition, Met. Chem.* **2009** 34, 593.
27. Soto-Garrido, G.; Salas-Reyes, V. *Transition Met. Chem.* **2000**, 25, 192.
28. Khandar, A.A.; Shaabani, B.; Belaj, F.; Bakhtiari, A. *Polyhedron* **2006**, 25, 1893.

29. Chen, H.; Han, D.; Yan, H.; Tang, W.; Yang, Y.;, Yang, W. *Acta Cryst.* **1996**, C52, 2204.
30. Sato, S.; Fukuda, T.; Ishii, K.; Nakano, Y.; Fujii, Y. *Acta Cryst.* **1999**, C55, 1466.
31. Meghdadi, S.; Mahmoudkhani, A.H. *Acta Cryst.* **2006**, E62, m69.
32. You, Z.-L.; Qu, Y.; Liu, W.-S.; Tan, M.-Y.; Zhu, H.-L. *Acta Cryst.* **2003**, E59, m1038.
33. Sun, Y.-X. *Acta Cryst.* **2005**, E61, m39.
34. Li, S.-Y.; You, Z.-L.; Chen, B.; Lin, Y.-S.; Xiong, Z.-D.; Zhu, H.-L. *Acta Cryst.* **2004**, E60, m999.
35. You, Z.-L.; Zhu, H.-L.; Liu, W.-S. *Acta Cryst.* **2004**, E60, m587.
36. Yang, M.-H.; Li, Y.-Z.; Zhu, C.-J.; Pan, Y.; Liu S.-H. *Acta Cryst.* **2004**, E60, o2397.
37. Yoon, J.W.; Yoon, T.-S.; Shin, W. *Acta Cryst.* **1997**, C53, 1685.
38. Mantero, D.G.; Altaf, M.; Neels, A.; Stoeckli-Evans, H. *Acta Cryst.* **2006**, E62, o5204.
39. Kuroda, R.; Saito, Y. *Acta Cryst.* **1974**, B30, 2126.
40. Sağlam, A.; Ucun, F.; Güçlü, V. *Spectrochim. Acta Part A* **2007**, 67, 465.
41. Pui, A.; Policar, C.; Mahy, J.P. *Inorg. Chim. Acta* **2007**, 360, 2139.
42. Avcı, D.; Atalay, Y.; Şekerci, M.; Dinçer, M. *Spectrochim. Acta Part A* **2009**, 73, 212.
43. Parimala, S.; Gita, K.N.; Kandaswamy, M. *Polyhedron* **1998**, 17, 3445.
44. Sanmartín, J.; García-Deibe, A.M.; Fondo, M.; Navarro, D.; Bermejo, M.R. *Polyhedron* **2004**, 23, 963.
45. Ware, D.C.; Mackie, D.S.; Brothers, P.J.; Denny, W.A. *Polyhedron* **1995**, 14, 1641.